



**HAL**  
open science

## Spectral mapping method based on intervals of comonotonicity for modelling of radiative transfer in non-uniform gaseous media

Frédéric André, Vladimir Solovjov, Brent W Webb, Mathieu Galtier, Philippe Dubuisson

► **To cite this version:**

Frédéric André, Vladimir Solovjov, Brent W Webb, Mathieu Galtier, Philippe Dubuisson. Spectral mapping method based on intervals of comonotonicity for modelling of radiative transfer in non-uniform gaseous media. *Journal of Quantitative Spectroscopy and Radiative Transfer*, 2019, 229, pp.33-39. 10.1016/j.jqsrt.2019.02.030 . hal-02090686

**HAL Id: hal-02090686**

**<https://hal.science/hal-02090686>**

Submitted on 23 Apr 2019

**HAL** is a multi-disciplinary open access archive for the deposit and dissemination of scientific research documents, whether they are published or not. The documents may come from teaching and research institutions in France or abroad, or from public or private research centers.

L'archive ouverte pluridisciplinaire **HAL**, est destinée au dépôt et à la diffusion de documents scientifiques de niveau recherche, publiés ou non, émanant des établissements d'enseignement et de recherche français ou étrangers, des laboratoires publics ou privés.

**SPECTRAL MAPPING METHOD BASED ON  
INTERVALS OF COMONOTONICITY FOR  
MODELLING OF RADIATIVE TRANSFER IN  
NON-UNIFORM GASEOUS MEDIA**

**Frédéric ANDRE<sup>\*1</sup>, Vladimir P. SOLOVJOV<sup>2</sup>, Brent W. WEBB<sup>2</sup>, Mathieu GALTIER<sup>1</sup>,  
Philippe DUBUISSON<sup>3</sup>**

<sup>1</sup> Univ Lyon, CNRS, INSA-Lyon, Université Claude Bernard Lyon 1, CETHIL UMR5008, F-69621 Villeurbanne, France

<sup>2</sup> Brigham Young University, 350G EB, Provo, UT 84602 USA

<sup>3</sup> Laboratoire d'Optique Atmosphérique, Univ. Lille – 5900 Lille, France

\* Corresponding author: frederic.andre@insa-lyon.fr.

**ABSTRACT.** The aim of this work is to describe a Spectral Mapping Method (SMM) to split spectral intervals into smaller sets of wavenumbers, called intervals of comonotonicity, over which gas spectra in distinct states are rigorously linked through a strictly increasing function. Over small intervals of comonotonicity, the proposed method becomes, in theory, exact. The step-by-step process of construction of intervals of comonotonicity is described and explained. The present work focuses on the two-cell problem. Despite its full generality for the treatment of the blurring effect in  $k$ -distribution approaches, the strength of the method is illustrated: 1/ with a high number of subintervals on an IR signature configuration, widely recognized as among the most challenging in band model theory; 2/ with only two subintervals, in a highly non-uniform two-cell configuration. Comparisons with reference Line-By-Line calculations and a mapping technique founded on a scaled map illustrate its relevance for radiative heat transfer and spectroscopic applications.

**KEYWORDS:** gas radiation, non-uniform, spectral mapping method (SMM), intervals of comonotonicity, comonotonic spectra,  $Ck$ , CKD.

## **NOMENCLATURE**

$g$  cumulative  $k$ -distribution – Eq. (1)

$k$  absorption coefficient ( $\text{cm}^{-1}$ )

$u$  abscissa at the origin for the lines used to split the  $g$ - $g$  plot (Sections 2 and 3)

$u$  scaling coefficient (Section 4)

### **Greek symbols**

$\Delta\eta$  spectral band width ( $\text{cm}^{-1}$ )

$\kappa_\eta$  spectral absorption coefficient ( $\text{cm}^{-1}$ )

$\varphi$  spectral mapping function ( $\text{cm}^{-1}$ )

$\eta$  wavenumber ( $\text{cm}^{-1}$ )

### **Subscripts / superscript**

1,2 relative to the thermophysical state 1 or 2 of the gas

## 1. INTRODUCTION

Extension of approximate models of gas radiation from uniform to non-uniform paths is among the most difficult problems in gas radiation modeling [1]. Although many methods are accurate enough for radiative heat transfer applications, most of them do not permit to achieve a precision sufficient for narrow and wide band spectroscopic (environmental, etc.) applications. In these cases, advanced techniques to improve approximate models of gas radiation for general non-uniform applications are required. These techniques can be organized in two main categories: Multiple-Line-Group methods [1] and Spectral Mapping techniques.

Multiple-Line-Group (MLG) approaches are among the oldest techniques. They first appeared in 1962 as part of Wyatt's quasi-random band model [2], and consist of an explicit grouping of spectral lines according to values of their linestrengths. The idea of combining spectral lines with similar lower state energy levels appeared in the 70s, as a way to ameliorate the treatment of highly non-isothermal paths. Early methods based on this idea are described in Refs. [3-6]. Recent appellations for these approaches are the fictitious gases [7] and the multi-scale method described in Baradwaj and Modest [8]. The method presented in Ref. [8] mostly reformulates in different words the approach proposed a few years earlier in Ref. [9]. The output of a MLG treatment is a set of groups of spectral lines whose centers are assumed to be statistically independent, from one group to another.

Spectral Mapping Methods (SMM) seek to avoid the use of simplifying assumptions to treat non-uniform gaseous paths (constant absorption coefficient, scaling, etc.) by iteratively splitting the spectral interval associated with the model's definition into sub-intervals over which these non-uniform treatments are not assumptions but actual properties of gas spectra. The output of a SMM treatment is a set of spectral intervals over which a particular relationship between high resolution spectra in distinct states (scaling, correlation / comonotonicity, etc.) can be assumed to be exact. Any SMM thus leads to some simplifications in the treatment of path non-

uniformities. Application of SMM requires high resolution spectral data, which explains why these techniques are more recent than MLG. The first SMM was in fact proposed by West and Crisp in 1990 [10]. It consists in building sub-intervals, or bins, in such a way that gas spectra are constant over the bins at each spatial location along non-uniform paths. This technique was improved recently in Refs. [11,12]. Other methods produce intervals over which gas spectra can be treated as scaled. Modest and co-workers' multi-group (MG) [13] (not to be confused with Ludwig's [3] or Khodyko / Vitkin [4-6] multi-group methods which are both founded on MLG) and multi-spectral techniques [14-17] fall in this category and differ principally by the way the spectral intervals are built. In two recent papers [18,19], efforts were made by Hu and Wang to improve the grouping scheme used in the Multi-Scale Multi-Group (MSMG) method of Modest by attempting to replace constraints on scaling coefficients, as used in the original version, by pragmatic criteria based on a correlated view. The necessity to treat differently single species and mixtures is closely related to the initial choice made by the authors to apply the MSMG method for their problem.

When formulated and applied properly, both MLG and SMM have the potential to improve significantly the treatment of path non-uniformities. No combinations of the two techniques, which are by construction redundant, are in this case required.

This work proposes a SMM technique that allows the building of spectral intervals over which gas spectra in distinct states are rigorously linked through a strictly increasing function. Accordingly, over these intervals that will be from now on referred to as intervals of comonotonicity, the two spectra at the distinct states can be related through monotonically increasing functions: spectra are called comonotonic [20], and the  $Ck$  / CKD approaches are exact. Notice that  $Ck$  and CKD acronyms represent the same method (the so-called Correlated approximation applied within the frame of the  $k$ -distribution technique) but one of them is

mostly encountered in Mechanical Engineering ( $Ck$ ) whereas the other one is more usual in Atmospheric Sciences (CKD).

The present method improves  $k$ -distribution methods by directly addressing the blurring effect of non-uniform  $k$ -distribution approximations: this effect is encountered both for high temperature (as considered here for illustration) and atmospheric applications. The simplification of the treatment of path non-uniformities that is provided by the present SMM results from the construction of spectral intervals over which this blurring effect can be effectively eliminated. The step-by-step process to construct intervals of rigorous comonotonicity, and thus “correlation” or “zero-blurring”, is described. It is applied here to narrow spectral intervals but its extension to any band width is possible since it only requires the specification of the cumulative  $k$ -distributions of the gas in distinct states: any particularity of the problem under study (width of the band, possible influence of optical filters and / or non-constant blackbody function) is already included in the calculation of the cumulative  $k$ -distribution. Application of the method to highly non-uniform situations, one of which is representative of the classically challenging IR plume signature calculation, illustrates the relevance of the method. The present grouping scheme can be used alone, as proposed here, or together with other techniques for which it can provide a relevant initial guess at the earliest stage of their iterative process.

## 2. BUILDING INTERVALS OF COMONOTONICITY

Let us consider two gas spectra at two distinct thermophysical states for which the spectral absorption coefficients in the two states are  $\kappa_{\eta}^1$  and  $\kappa_{\eta}^2$ , respectively. The cumulative  $k$ -distribution functions that correspond to these two spectra are:

$$g_i(k_i) = \frac{1}{\Delta\eta} \cdot \int_{\Delta\eta} H(k_i - \kappa_{\eta}^i) d\eta, \quad i=1,2 \quad (1)$$

where  $H$  is the Heaviside step function. The problem is formulated here within the frame of narrow band approaches but can be extended to any other band, up to the full spectrum, by replacing  $d\eta/\Delta\eta$  in Eq. (1) by any weighting function of the form  $\omega(\eta) d\eta$  where  $\omega(\eta) > 0$  and  $\int \omega(\eta) d\eta = 1$ .

We start our analysis by plotting the absorption spectra for the two thermophysical states not as functions of wavenumbers, as in usual LBL representations, but with respect to the cumulative distribution function of the absorption coefficient in State 1,  $g_1(\kappa_\eta^1)$ . State 1 is a 1 % H<sub>2</sub>O – 99 % N<sub>2</sub> mixture at 300 K ; State 2 is 10 % H<sub>2</sub>O – 90 % N<sub>2</sub> at 1500 K. The 25 cm<sup>-1</sup> narrow band considered for the following figures is centered at 3400 cm<sup>-1</sup>, in the 2.7 μm band of H<sub>2</sub>O. This spectral region is widely used in IR plume signature studies [9,21].

For this purpose, we start with the high resolution (10<sup>-2</sup> cm<sup>-1</sup>) spectra in the two states, provided as vectors  $(\kappa_{\eta_1}^1, \kappa_{\eta_2}^1, \dots, \kappa_{\eta_N}^1)$  and  $(\kappa_{\eta_1}^2, \kappa_{\eta_2}^2, \dots, \kappa_{\eta_N}^2)$  where  $(\eta_1, \eta_2, \dots, \eta_N)$  is the set of wavenumbers used in the LBL calculation, and calculate two new vectors  $(g_1(\kappa_{\eta_1}^1), g_1(\kappa_{\eta_2}^1), \dots, g_1(\kappa_{\eta_N}^1))$  and  $(g_2(\kappa_{\eta_1}^2), g_2(\kappa_{\eta_2}^2), \dots, g_2(\kappa_{\eta_N}^2))$  by application of Eq. (1). If one sets  $(g_1(\kappa_{\eta_1}^1), g_1(\kappa_{\eta_2}^1), \dots, g_1(\kappa_{\eta_N}^1))$  as abscissa axis and plots  $(\kappa_{\eta_1}^1, \kappa_{\eta_2}^1, \dots, \kappa_{\eta_N}^1)$  and  $(\kappa_{\eta_1}^2, \kappa_{\eta_2}^2, \dots, \kappa_{\eta_N}^2)$  with respect to this vector, one receives Figure 1.

After the change of abscissa axis from wavenumbers to  $g_1(\kappa_\eta^1)$ , the gas spectrum in State 1 is monotonically increasing (this is the main principle of the  $k$ -distribution method) whereas the absorption spectrum in State 2 is not (in the present case but this observation is rather general) an increasing function of  $g_1(\kappa_\eta^1)$ . This departure from monotonicity is the main source of error in the  $Ck$  / CKD approaches.



Our aim is to build spectral intervals over which gas spectra are comonotonic viz. to extract subsets of points from the cloud of circles (absorption coefficient in State 2 reorganized with respect to  $g_1(\kappa_\eta^1)$  - in other words, values of  $\kappa_\eta^2$  at the wavenumbers  $\eta$  where  $\kappa_\eta^1$  is associated with the pseudo-spectral wavenumber  $g_1(\kappa_\eta^1)$ ) of Figure 1 that increase with respect to  $g_1$ .

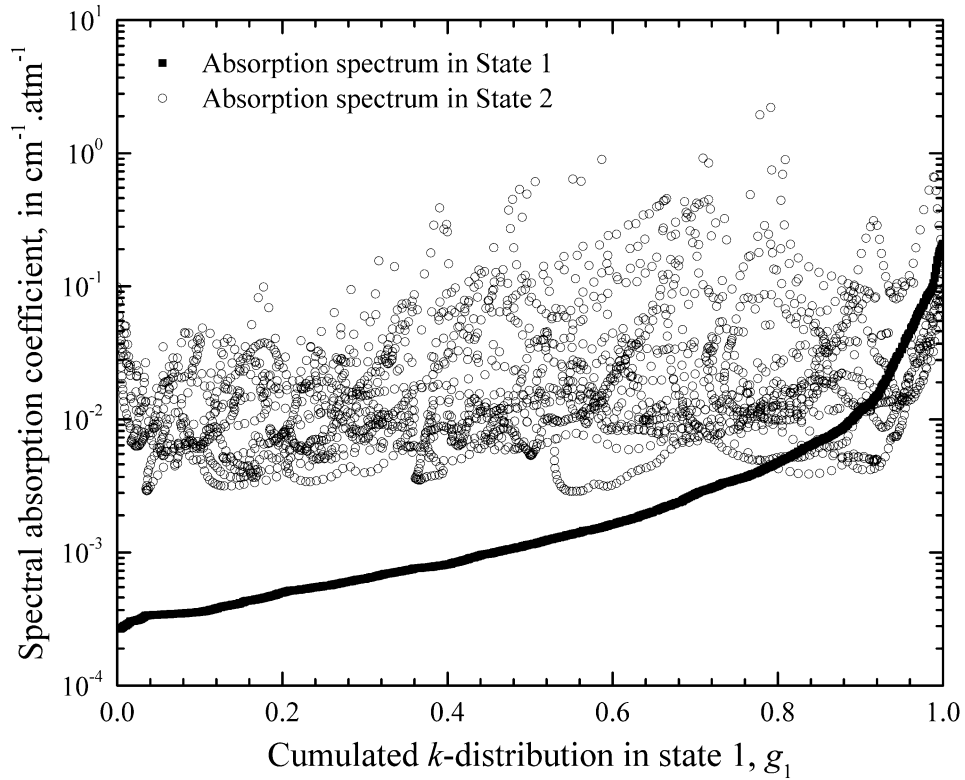


**Figure 1.** Example of two spectra reordered with respect to the same (related to State 1) cumulative  $k$ -distribution function. Gas spectra are clearly not comonotonic / correlated.

For this purpose, we will mostly follow the same steps as in Ref. [15] where the objective was to construct sub-intervals over which gas spectra are scaled. However, the starting point is slightly different. Indeed, the main difference between the two approaches (scaled in [15] or correlated / comonotonic here) is that we will replace the  $C$ -curves of Ref. [15] (2-dimensional parametric curve  $k_1 = \kappa_\eta^1$ ,  $k_2 = \kappa_\eta^2$  in the  $(k_1, k_2)$ -plane) by a  $g$ - $g$  plot (2-dimensional parametric

plot of  $g_1 = g_1(\kappa_\eta^1)$ ,  $g_2 = g_2(\kappa_\eta^2)$  in the  $(g_1, g_2)$ -plane). This kind of representation is not new in the radiative heat transfer literature and can be found for instance in Ref. [22] to illustrate the blurring effect of  $k$ -distribution methods viz. to show their possible departure from the so-called “correlated” assumption. An example of  $g$ - $g$  plot is given in Figure 2 corresponding to the same set of LBL data as for Figure 1. This figure was obtained by setting  $(g_1(\kappa_{\eta_1}^1), g_1(\kappa_{\eta_2}^1), \dots, g_1(\kappa_{\eta_N}^1))$  as abscissa axis and plotting  $(g_2(\kappa_{\eta_1}^2), g_2(\kappa_{\eta_2}^2), \dots, g_2(\kappa_{\eta_N}^2))$  with respect to  $g_1 = g_1(\kappa_\eta^1)$ . For the sake of legibility, only the points associated with the discrete wavenumbers used in the LBL calculation of  $\kappa_\eta^1$  and  $\kappa_\eta^2$  are depicted.

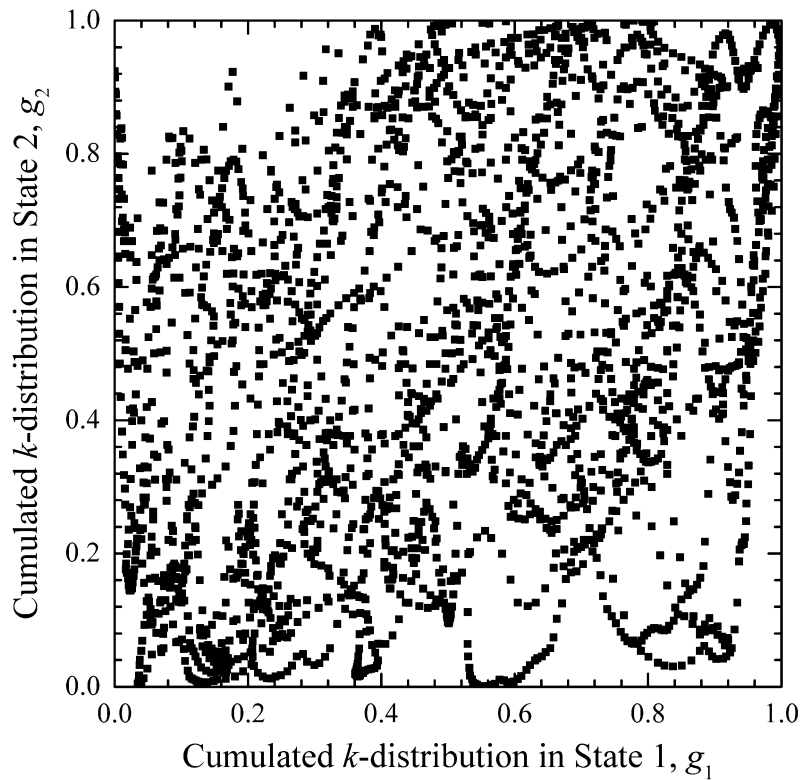


**Figure 2.** Example of  $g$ - $g$  plot (same case as Figure 1)

Figure 3 represents a simplified model of  $g$ - $g$  plot. If gas spectra were actually ‘‘correlated’’, their cumulative distribution would take equal values at all wavenumbers and all the points  $g_1 = g_1(\kappa_\eta^1)$ ,  $g_2 = g_2(\kappa_\eta^2)$  would be aligned on the straight diagonal line  $D_0$ . As gas spectra are not correlated / comonotonic in the case considered, points of coordinates  $g_1 = g_1(\kappa_\eta^1)$ ,  $g_2 = g_2(\kappa_\eta^2)$  can be found in various regions of the unit square. The building of sub-intervals of comonotonicity consists in splitting the unit square in a pertinent way so as to define these intervals. In other words, we seek to identify using Fig. 2 wavenumber intervals where the two spectra are related through a strictly increasing function, viz. over which they share the same monotonicity by increasing or decreasing simultaneously.

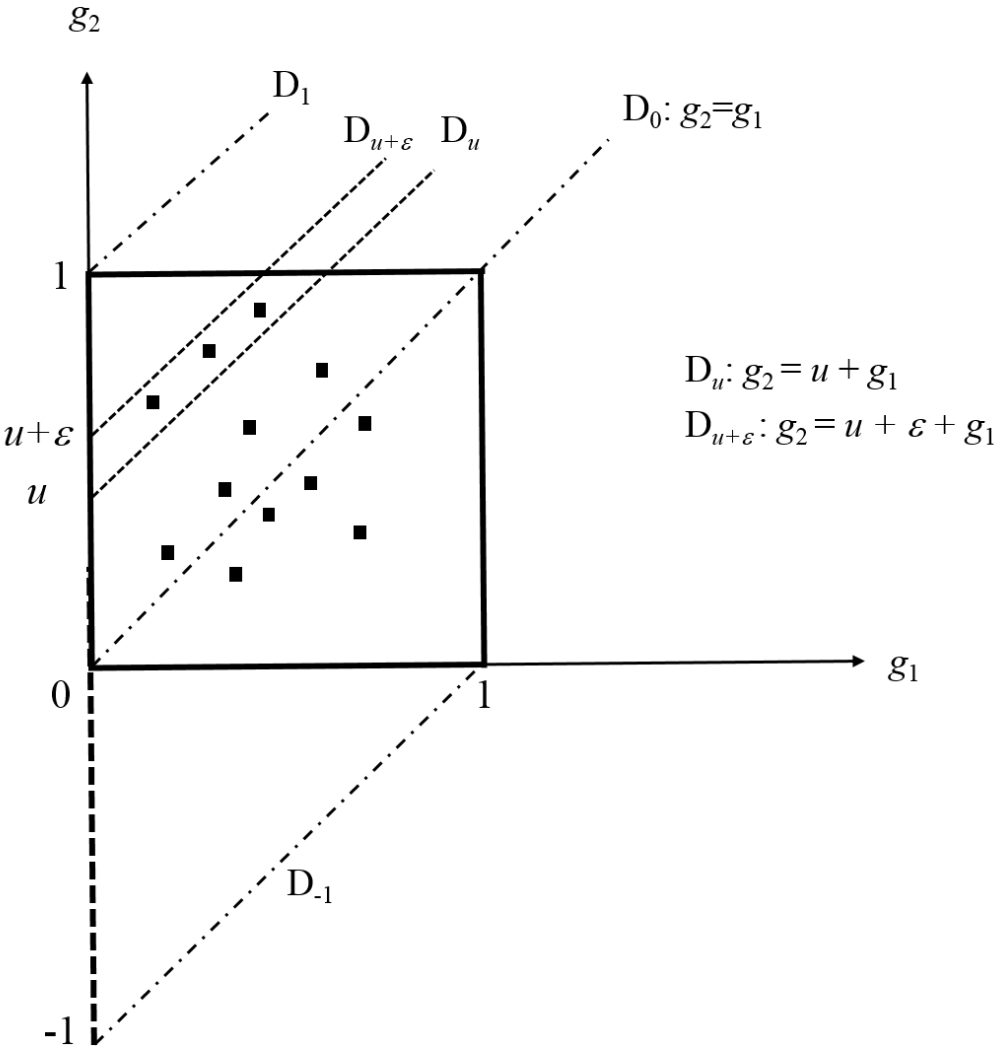


**Figure 3.** Schematic representation of a  $g$ - $g$  plot

Let us focus our attention on the set of wavenumbers  $\Delta\eta(u)$  built by grouping together the points located between the two lines  $D_u$  and  $D_{u+\varepsilon}$ , where  $\varepsilon$  is a positive increment and  $u$  takes values between -1 and 1. At all these spectral locations, one has:

$$u < g_2(\kappa_\eta^2) - g_1(\kappa_\eta^1) < u + \varepsilon \quad (2)$$

Consequently, for small increments  $\varepsilon$ , all the values of the absorption coefficient in State 2 over  $\Delta\eta(u)$  are associated with values of the absorption coefficient in State 1 through the following linear relationship:

$$g_2(\kappa_\eta^2) \approx u + g_1(\kappa_\eta^1), \quad \eta \in \Delta\eta(u) \quad (3)$$

or equivalently:

$$\kappa_\eta^2 = g_2^{-1}[u + g_1(\kappa_\eta^1)] = \varphi_u(\kappa_\eta^1), \quad \text{where } \varphi_u(k) = g_2^{-1}[u + g_1(k)] \quad (4)$$

Eq. (4) shows that the two absorption spectra  $\kappa_\eta^1$  and  $\kappa_\eta^2$  are linked to each other through a strictly increasing function  $\varphi_u$ , that depends on  $u$ , at all spectral locations  $\eta \in \Delta\eta(u)$ .

In this case, the cumulative- $k$  distributions restricted to the interval  $\Delta\eta(u)$  which are defined for the two states 1 and 2 as:

$$g_i[k_i | \Delta\eta(u)] = \frac{1}{\Delta\eta(u)} \cdot \int_{\Delta\eta(u)} H(k_i - \kappa_\eta^i) d\eta, \quad i=1,2 \quad (5)$$

take equal values for any wavenumber inside  $\Delta\eta(u)$  and follow rigorously:

$$g_1[\kappa_\eta^1 | \Delta\eta(u)] = g_2[\kappa_\eta^2 | \Delta\eta(u)], \quad \eta \in \Delta\eta(u) \quad (6)$$

This relationship arises directly from the equalities Eqs. (3,4) and the definition of comonotonicity, viz. two variables are comonotonic if and only if they can be linked to each

other through a strictly increasing function in which case their rank / cumulative distribution functions are equal [20]. Intervals  $\Delta\eta(u)$  thus correspond to intervals of comonotonicity, i.e., spectral intervals over which gas spectra are comonotonic.

Based on the same principle, the unit square can be discretized into diagonal belts at fixed values of  $u$ . All the points that belong simultaneously to the  $g$ - $g$  plot and a given belt can then be grouped to define a spectral interval over which gas spectra are comonotonic and, consequently, over which the  $Ck$  / CKD method is exact. By varying the parameter  $u$  between -1 and 1 one reconstructs the unit square and thus the set of wavenumbers (the narrow band considered in this work)  $\Delta\eta$ .

### 3. APPLICATION

The results provided in this section are based on the same LBL dataset as described in Ref. [15]. They use spectral line parameters taken from HITEMP2010 [23] as inputs. The two states considered in this section are the same as for the previous figures: State 1 is a 1 % H<sub>2</sub>O – 99 % N<sub>2</sub> mixture at 300 K ; State 2 is 10 % H<sub>2</sub>O – 90 % N<sub>2</sub> at 1500 K. As noticed earlier, spectra were restricted to the 25 cm<sup>-1</sup> spectral band centered at 3400 cm<sup>-1</sup> for Figures 1,2,4,5.

Building intervals of comonotonicity from the sets of vectors described in the previous section up to radiative heat transfer calculations requires several steps:

A / the first step consists of splitting the  $g$ - $g$  plot of Figure 2 into different diagonal belts, each of which corresponds to a distinct value of the parameter  $u$ . The splitting process was done by:

1/ evaluating the distribution function  $F$  of the spectral variable  $g_2(\kappa_\eta^2) - g_1(\kappa_\eta^1)$ ; 2/ dividing the unit interval  $[0,1]$  into  $N + 1$  equally spaced values  $X_i$ ,  $i = 1, N + 1$ ;  $X_1 = 0$ ;  $X_{N+1} = 1$  ; 3/ solving  $F(u_i) = X_i$  to define bounds  $u_i$ ,  $i = 1, N + 1$  for the variable  $u$ ; 4/ the  $i$ -th belt then consists of all wavenumbers for which  $u_i \leq g_2(\kappa_\eta^2) - g_1(\kappa_\eta^1) \leq u_{i+1}$ .

In this section,  $N = 25$  belts were constructed by this method. Each belt contains roughly the same number of points ( $100 \pm 2$  spectral values of the absorption coefficients). Results (only a few subsets are plotted for legibility) are depicted in Figure 4.

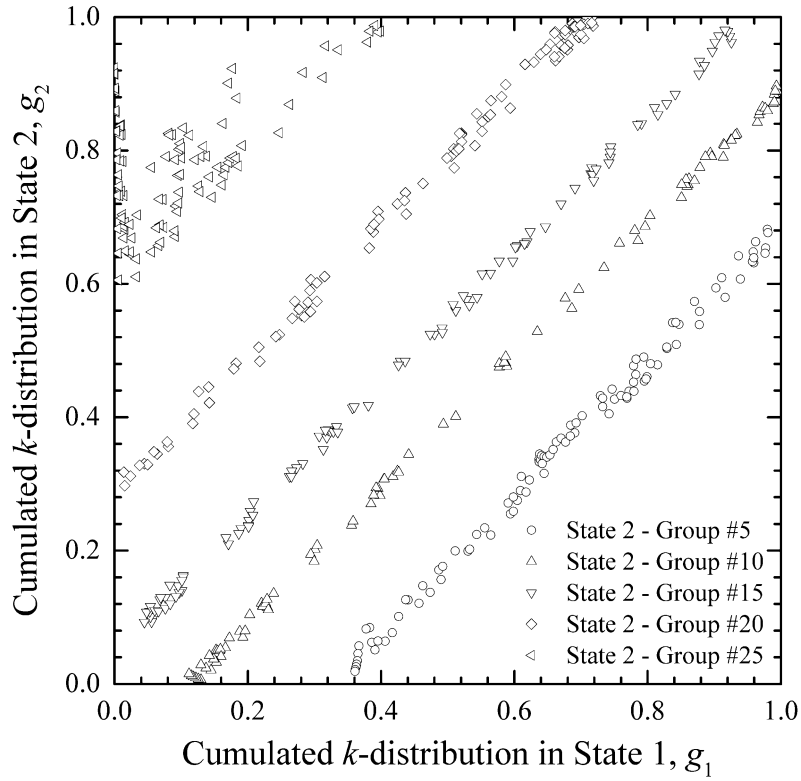


**Figure 4.** Discretization of the  $g$ - $g$  plot into diagonal belts

B/ Next, all the points inside a diagonal belt, made of many noncontiguous intervals, are prescribed to the same group. This defines an ensemble of  $N = 25$  groups together with their corresponding intervals  $\Delta\eta(u)$ ,  $u \in (-1,1)$ . An inverse transformation  $g_2^{-1}$  is then applied to all the elements in each group and the corresponding absorption coefficients are plotted with the same symbols as in the  $g$ - $g$  plot of Figure 4. This yields Figure 5. The simple process described in the previous section clearly allows extracting from the cloud of points depicted in

Figure 1 subsets of  $k$ -values that almost share the same monotonicity with respect to  $g_1$  in the two states.

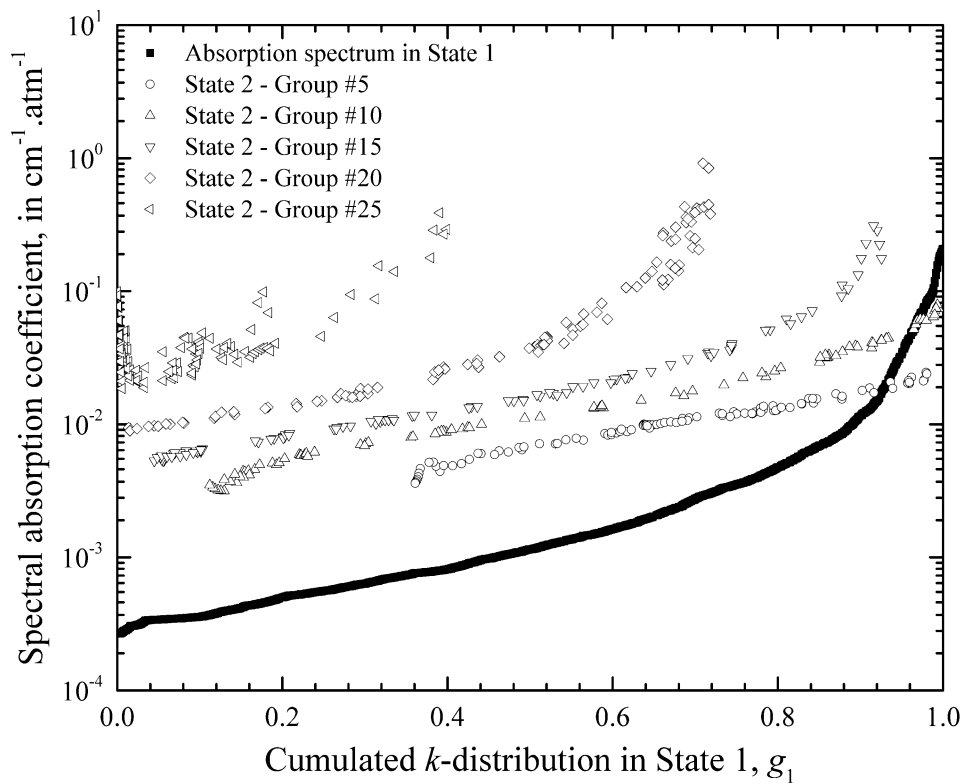


**Figure 5.** Subsets of comonotonic absorption coefficients (groups)

C/ In the final step, each set of absorption coefficients in a group of wavenumber  $\eta \in \Delta\eta(u)$  is treated as an independent spectrum over which a  $k$ -distribution parameterization is applied viz. a distribution function is evaluated over the set of  $k$ -values inside a belt  $\Delta\eta(u)$  and then inverted to provide an ensemble of corresponding gray gas absorption coefficients. Outcomes of this method are plotted in Figures 6 and 7. These figures correspond to a plume signature situation. For the narrow band averaged IR plume signature calculation of Figure 6, the length of the cold (State 1) path is 1000 m and that of the hot path (State 2) is 80 cm. Gases are at atmospheric pressure. Figure 6 shows the predicted radiative intensity exiting the cold layer and Figure 7 depicts the normalized errors on intensities calculated by the approximate models and

reference LBL calculations. For comparison purposes, results of a  $Ck-1$  model ( $Ck$  / CKD model built on  $1\text{ cm}^{-1}$  wide spectral intervals) averaged over  $25\text{ cm}^{-1}$  are also provided together with a  $Ck-25$  model ( $Ck$  / CKD model built on  $25\text{ cm}^{-1}$  wide spectral intervals). The two approaches ( $Ck-1$  and the  $Ck$  model based on intervals of comonotonicity) use weights and nodes based on a 7<sup>th</sup> order Gauss-Legendre quadrature and thus share the same computational cost after the belts of comonotonicity are determined. The  $Ck-25$  model uses the same type of quadrature at order 25. The approximation based on the intervals of comonotonicity clearly outperforms that obtained with a discretization of the  $25\text{ cm}^{-1}$  narrow bands into contiguous spectral intervals, viz.  $Ck-1$ .

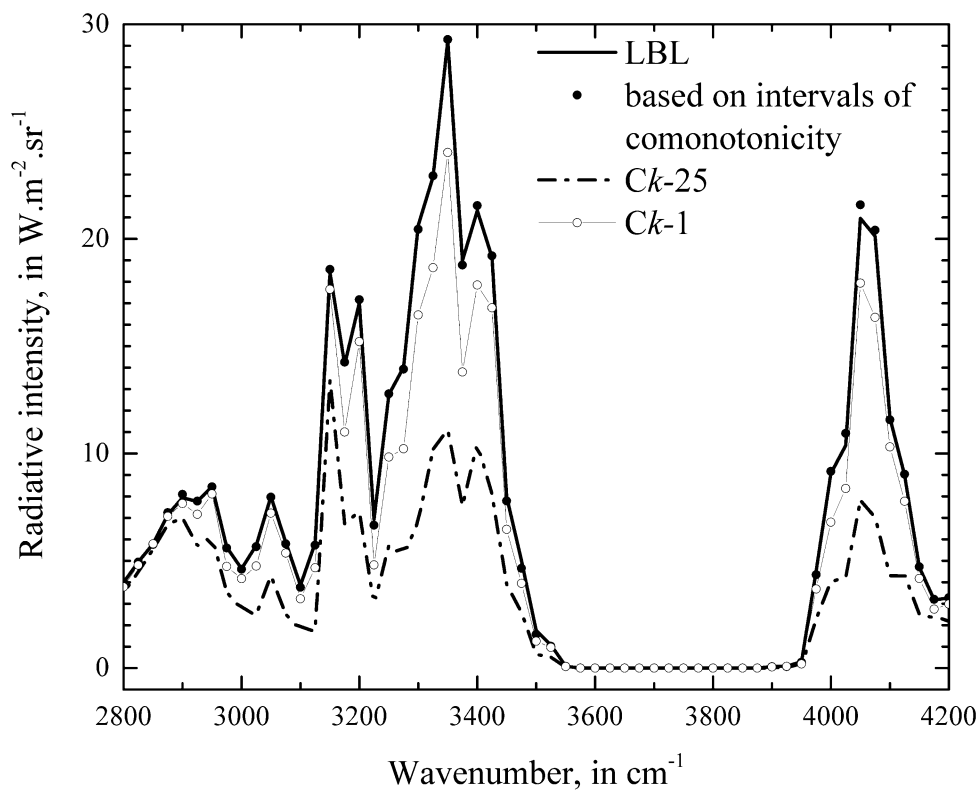


**Figure 6.** Radiative intensity at the exit of the cold path



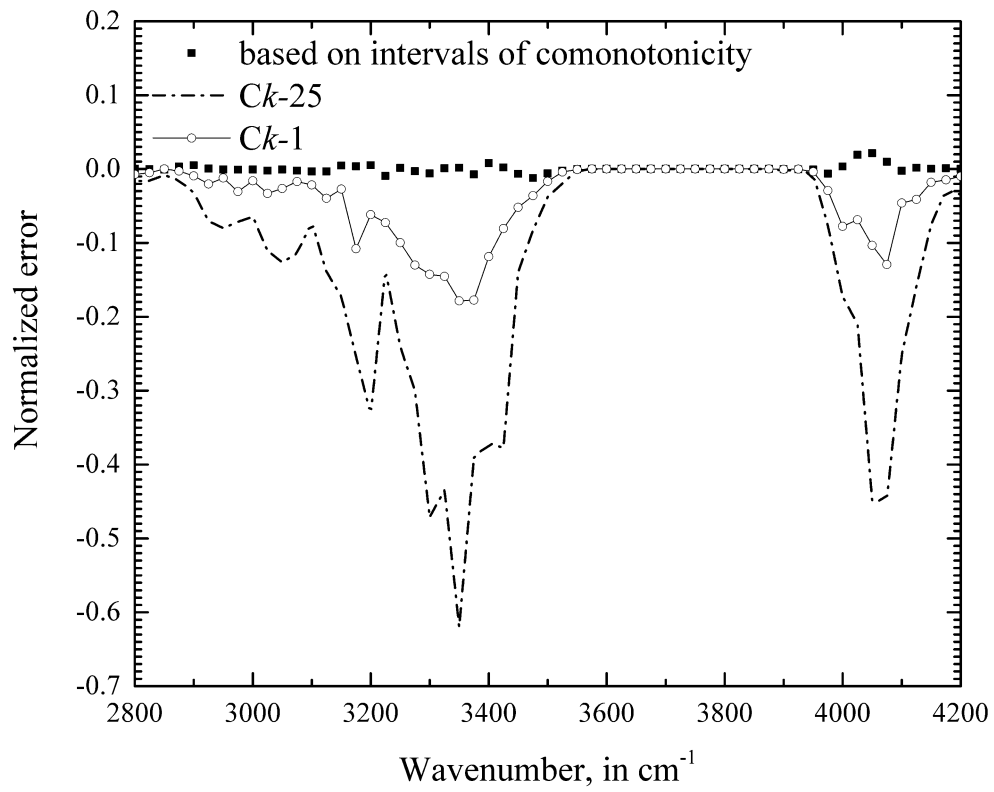


**Figure 7.** same as Figure 6 but expressed as the normalized error defined as the difference Model intensity – LBL intensity divided by the maximum intensity over the spectral range  $[2800 \text{ cm}^{-1}, 4200 \text{ cm}^{-1}]$

#### 4. COMPARISON WITH A MAPPING TECHNIQUE BASED ON INTERVALS OF SCALING

As emphasized in the introduction, there exist many mapping methods in the literature to improve approximate models of gas radiation in non-uniform situations. Among them, techniques based on intervals of scaling are probably the simplest. They are all built on the same simple idea, explained below.

At high spectral resolution, gas spectra are rigorously scaled. However, the scaling property cannot, in general, be extended to spectral bands since, for any two absorption spectra  $\kappa_\eta^1$  and  $\kappa_\eta^2$  of the same molecule in distinct states, the ratio  $u_\eta = \kappa_\eta^2 / \kappa_\eta^1$  is rarely a constant over a contiguous set of wavenumbers of non-null width  $\Delta\eta$ . One can however define, as for  $\kappa_\eta^1$  and  $\kappa_\eta^2$ , a distribution function for this new spectral variable  $u_\eta = \kappa_\eta^2 / \kappa_\eta^1$  :

$$F(u) = \frac{1}{\Delta\eta} \cdot \int_{\Delta\eta} H(u - u_\eta) d\eta = \mathbb{P}(u_\eta < u) \quad (7)$$

This distribution function can be used to define intervals of scaling. Indeed, they can be built by application of the following steps: 1/ the unit interval  $[0,1]$  is divided into  $N + 1$  equally spaced values  $X_i$ ,  $i=1, N+1$ ;  $X_1=0$ ;  $X_{N+1}=1$  ; 2/  $F(u_i) = X_i$  is solved, where  $F$  is now given by Eq. (7) and represents the distribution function of scaling coefficients, which provides bounds  $u_i$ ,  $i=1, N+1$  for the variable  $u_\eta = \kappa_\eta^2 / \kappa_\eta^1$  ; 3/ subintervals are then obtained by grouping together all wavenumbers for which  $u_i \leq \frac{\kappa_\eta^2}{\kappa_\eta^1} \leq u_{i+1}$ ; 4/ over these intervals, the ratio  $u_\eta = \kappa_\eta^2 / \kappa_\eta^1$  is roughly a constant (in the same way that when applied directly to gas spectra the method provides gray gases). Absorption spectra can thus be treated as scaled (their ratio is a constant) over the corresponding sets of wavenumbers.

It can be noticed that for large  $N$ , a constant value of the ratio of the two spectra is a fair approximation inside each of the subintervals provided by this method so that a mean scaling coefficient can be realistically introduced. For small values of  $N$ , however, the use of the  $Ck$  / CKD method can correct errors due to non-constant scaling coefficients and should be preferred, as suggested in Ref. [13]. This is the method selected in this section since the choice  $N=2$  was made. Indeed, since the two methods that we want to compare (based on intervals of scaling or comonotonicity) converge toward the exact solution at infinite values of  $N$ , their comparison only has relevance for small values of  $N$ . Notice also that the two methods based on intervals of scaling and comonotonicity share in this case almost the same RTE solver. Only the intervals used to construct conditional (viz. restricted to subintervals, as introduced in Eq. (5) for the comonotonic case)  $k$ -distribution functions differ.

This method to construct intervals of scaling is not exactly the same as used, for instance, by Zhang and Modest in the multi-group method [13] or in Refs. [14-17] for the multispectral approach, both of which use some criterion on spectral scaling coefficients over sequences of thermophysical states to construct intervals of scaling. Here, only two states are treated. However, these techniques are founded on the same principle (aggregate intervals in such a way that the ratio of any two spectra is a constant) and should provide, in theory, exactly the same results as those provided by the present method.

The two spectral mapping techniques (scaling / comonotonicity intervals) are compared and assessed against LBL calculation in a case taken from Ref. [13]. Results of a  $Ck$ -12.5 model and the spectral mapping method proposed by Zhang and Modest in [13], based on the arbitrary cut-off on scaling coefficients  $u_{cut-off} = 10$ , are also provided for completeness. The two cells contain the same gas, 20%  $H_2O$ , 80%  $N_2$  at atmospheric pressure. The hot layer is at 2000 K and its length is 50 cm, and the cold layer is at 300 K and its length varies. Calculations are made over narrow bands and then integrated over the full spectrum to provide total intensities

which are used for comparisons with LBL calculations. These intensities are evaluated at the cold side. Results are shown in Figure 8.

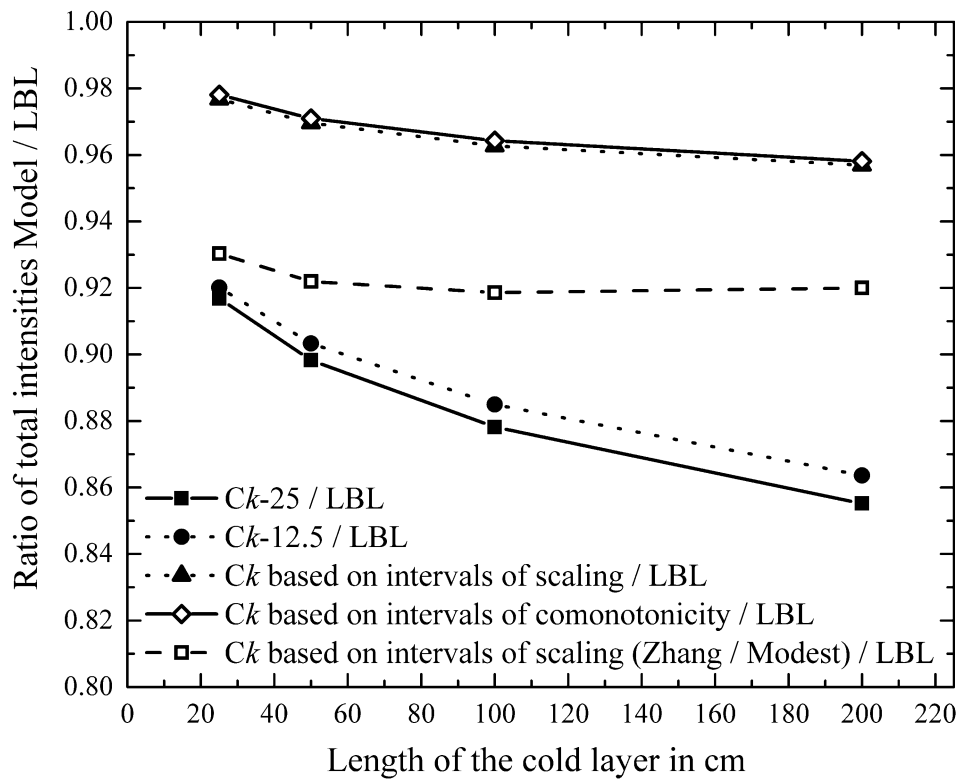


**Figure 8.** Comparison of several spectral mapping methods

From the results shown in Figure 8, the following conclusions can be drawn:

1/ Splitting the  $25 \text{ cm}^{-1}$  narrow band into two contiguous subintervals (yielding the  $Ck-12.5$  solid circles) does not improve the approximation significantly compared to the  $Ck-25$  method (solid squares).

2/ Using intervals of scaling or comonotonicity clearly yields a high gain in terms of accuracy, with errors reduced in the present case by a factor 4 when either the grouping scheme based on scaling or comonotonicity described in this work are used. At identical computational costs, spectral mapping methods have the potential to improve significantly the accuracy of the  $k$ -distribution methods compared to a crude splitting of the band into narrower sets. In the present

case, the model based on intervals of comonotonicity has a slightly higher accuracy than the model based on intervals of scaling. The spectral scaling method proposed by Zhang and Modest also improves the accuracy of narrow band calculations, but can clearly not compete in the case considered here with the two other grouping schemes described in this paper.

Finally, Figure 9 depicts mean Spearman's coefficients calculated over narrow bands. Spearman's coefficient is a measure of dependence [20] and characterizes the non-linear dependence between sets of values / random variables. The *Ck* / CKD model assumes this coefficient to be 1. A null value of Spearman's coefficient indicates complete statistical independence. Negative values can be observed when high values in a sequence are associated with low values in the other sequence, in which case variables are called counter-monotonic. Over a narrow band  $\Delta\eta$ , and for two thermophysical states as defined in section 2, Spearman's coefficient can be calculated as [24]:

$$\rho_{SP}(\kappa_{\eta}^1, \kappa_{\eta}^2) = 12 \cdot \frac{1}{\Delta\eta} \cdot \int_{\Delta\eta} g_1(\kappa_{\eta}^1) g_2(\kappa_{\eta}^2) d\eta - 3 \quad (8)$$

One can readily confirm that when spectra follow rigorously the implicit equation associated with so-called "correlated" models, this coefficient is actually 1. In the modern statistical literature [20], a Spearman's coefficient equal to 1 characterizes comonotonic variables.

Over sub-intervals, one can similarly define group Spearman's coefficients by simply replacing the full band  $\Delta\eta$  by the interval  $\Delta\eta(u_i)$ , where  $u_i$  is the quantity assumed to be fixed over the spectral interval and that can either represent a constraint on scaling or comonotonicity. It is then possible to calculate an average value by weighting the Spearman's coefficients over the groups by the fraction of the interval associated with each group. In the case of two groups, as considered in this section, one then obtains:

$$\left\{ \begin{array}{l} \overline{\rho_{\text{SP}}(\kappa_{\eta}^1, \kappa_{\eta}^2)} = \frac{\Delta\eta(u_1)}{\Delta\eta} \cdot \rho_{\text{SP},1}(\kappa_{\eta}^1, \kappa_{\eta}^2) + \frac{\Delta\eta(u_2)}{\Delta\eta} \cdot \rho_{\text{SP},2}(\kappa_{\eta}^1, \kappa_{\eta}^2) \\ \rho_{\text{SP},i}(\kappa_{\eta}^1, \kappa_{\eta}^2) = 12 \cdot \frac{1}{\Delta\eta(u_i)} \cdot \int_{\Delta\eta(u_i)} g_1(\kappa_{\eta}^1|u_i) g_2(\kappa_{\eta}^2|u_i) d\eta - 3 \end{array} \right. \quad (9)$$

These averaged Spearman's coefficients  $\overline{\rho_{\text{SP}}(\kappa_{\eta}^1, \kappa_{\eta}^2)}$  are plotted in Figure 9 for the same case as for Figure 8 and for the two grouping schemes discussed in this paper (Modest and Zhang's technique is not considered). For the *Ck* model, Spearman's coefficients were calculated from Eq. (8): low and even negative values are observed. This explains why the *Ck* / CKD method provides poor predictions in this high temperature gradient case, since the so-called "correlation" assumption is clearly inappropriate in this situation. Using the two grouping techniques described in this paper leads to higher values of averaged Spearman's coefficients  $\overline{\rho_{\text{SP}}(\kappa_{\eta}^1, \kappa_{\eta}^2)}$ , which explains why the radiative transfer results of Figure 8 are more in accordance with LBL calculations when these grouping schemes are used than with the narrow band *Ck* / CKD.

Notice also that averaged Spearman's coefficients are slightly higher in the comonotonic case than with scaling, which proves that the method to construct intervals of comonotonicity actually improves the monotonic relationship between spectral values over the groups. Furthermore, increasing the number of groups provides averaged Spearman's coefficients that approach unity: the relatively small values observed here are due to the choice of only two groups. Finally, observing distinct values for the sets of Spearman's coefficients proves that the two techniques, based on intervals of scaling or comonotonicity, yield overlapping though distinct sets of wavenumbers.

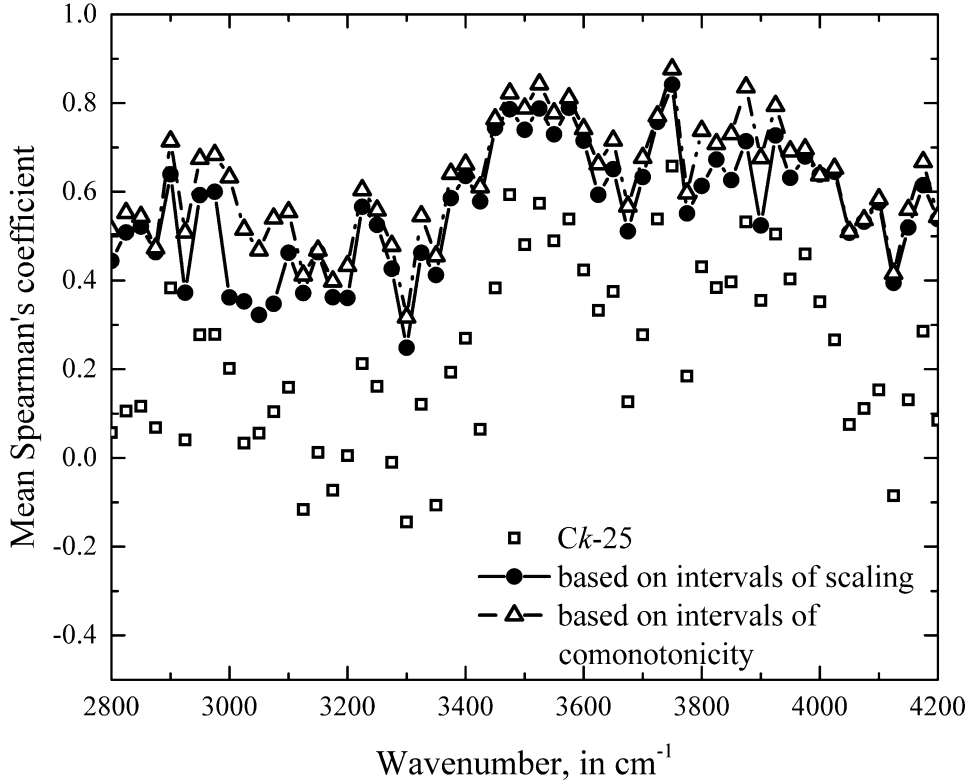


**Figure 9.** Comparison of averaged Spearman's coefficients for several spectral methods

## 5. CONCLUSION AND PERSPECTIVES

The method described in the present note to construct intervals of comonotonicity: 1/ is simple to understand and use, 2/ does not require an iterative process in the case of two-cell problems (its extension to more general situations is kept as future work), and 3/ can be applied over any band width, from narrow bands up to the full spectrum. It was shown to provide accurate predictions of radiative intensities in situations representative of IR plume signature configurations, a problem widely recognized as among the most complicated in band model theory. Comparisons with a *Ck* / CKD model based on intervals of scaling were also described and shown to provide a similar accuracy.

In addition, the method presented in this paper can be applied to atmospheric problems requiring accurate treatment of gaseous absorption, such as for radiative forcing calculations or remote sensing in absorbing bands. In this paper, the proposed method has been applied using

two thermophysical states including temperatures of 300 and 1500 / 2000 K. However, atmospheric applications cover a narrower range of temperature. In this respect, Fu and Liou [22] have presented  $g$ - $g$  plots for atmospheric conditions (temperature range between 245 and 300 K) and shown that the temperature effect produces more blurring. The degree of blurring is then weaker for atmospheric applications, with points less scattered around the diagonal line in the  $g$ - $g$  plot. The building of intervals of comonotonicity should then be easier to define, leading to reduced calculations times. The approach presented in this study is then a promising method to improve the  $k$ -distribution and to reduce errors associated with the  $Ck$  / CKD assumptions between atmospheric levels.

Finally, one can notice that no application of the Godson-Weinreb-Neuendorffer's (GWN) method [1] or use of effective scaling factors (see Ref. [24], in which a detailed analysis can be found) was considered in this paper. Such comparisons are scheduled as future work together with a comprehensive comparison of the two present techniques, extended to more than two cells, with the Mixture  $\ell$ -Distribution approach (MLD) viz. the  $\ell$ -distribution method [25] applied to intervals of scaling.

## ACKNOWLEDGEMENTS

This work has been supported by the Programme National de Télédétection Spatiale (PNTS, <http://www.insu.cnrs.fr/pnts> grant N° PNTS-2017-04).



## REFERENCES

- [1] YOUNG SJ. Band model theory of radiation transport, The Aerospace Press, 2013. ISBN: 978-1-884989-25-4.
- [2] WYATT PJ, STULL VR, PLASS GN. Quasi-random model of band absorption, *JOSA* 1962;52:1209-1217.
- [3] LUDWIG CB, MALKMUS W, REARDON JE, THOMPSON JAL. Handbook of infrared radiation from combustion gases, R GOULARD and JAL THOMPSON, eds, NASA SP-3080, 1973.
- [4] VITKIN EI, KABASHNIKOV VP, KMIT GI. New method of calculating the infrared emission of nonuniform volumes of molecular gases, *Zhurnal Prikladnoi Spektroskopii* 1979;30:686-693.
- [5] KHODYKO YV, VITKIN EI, KABASHNIKOV VP. Methods of calculating molecular-gas radiation on the basis of spectral-composition modelling, *Inzhenerno-Fizicheskii Zhurnal* 1979;36:204-217.
- [6] KHODYKO YV, KUSKOV AA, ANTIPOROVICH NV. Multigroup method for the calculation of selective IR radiation transfer in nonhomogeneous media, *Zhurnal Prikladnoi Spektroskopii* 1986;46:449-455.
- [7] LEVI DI LEON R, TAINE J. A fictive gas-method for accurate computation of low-resolution IR gas transmissivities: application to the 4.3  $\mu\text{m}$  CO<sub>2</sub> band, *Revue Phys. Appl.* 1986;21:825-831.
- [8] BHARADWAJ SP, MODEST MF. A multiscale Malkmus model for treatment of inhomogeneous gas paths, *Int J Thermal Sciences* 2007;46:479-490.

- [9] SOUFIANI A, ANDRE F, TAINE J. A fictitious-gas based statistical narrow-band model for IR long-range sensing of H<sub>2</sub>O at high temperature, *JQSRT* 2002;73:339-347.
- [10] WEST R, CRISP D, CHEN L. Mapping transformations for broadband atmospheric radiation calculations, *JQSRT* 1990;43:191-199.
- [11] BENNARTZ R, FISCHER J. A modified k-distribution approach applied to narrow band water vapor and oxygen absorption estimates in the near infrared, *JQSRT* 2000;66:539-553.
- [12] DOPPLER L, PREUSKER R, BENNARTZ R, FISCHER J. k-bin and k-IR: k-distribution methods without correlation approximation for non-fixed instrument response function and extension to the thermal infrared – applications to satellite remote sensing, *JQSRT* 2014;133:382-395.
- [13] ZHANG H, MODEST MF. Multi-group full-spectrum *k*-distribution database for water vapour mixtures in radiative transfer calculations, *IJHMT* 2003;46:3593-3603.
- [14] ANDRE F, HOU L, ROGER M, VAILLON R. The multispectral gas radiation modeling: a new theoretical framework based on a multidimensional approach to k-distribution methods, *JQSRT* 2014;147:178-195.
- [15] ANDRE F, HOU L, SOLOVJOV V.P. An exact formulation of *k*-distribution methods in non-uniform gaseous media and its approximate treatment within the Multi-Spectral framework, *Eurotherm Conference N°105: Computational Thermal Radiation in Participating Media V, 1-3 Avril 2015, Albi, France*.
- [16] ANDRE F, VAILLON R, GALIZZI C, GUO H, GICQUEL O. A multi-spectral reordering technique for the full spectrum SLMB modeling of radiative heat transfer in nonuniform gaseous mixtures, *JQSRT* 2011;112:394-411.

- [17] ANDRE F, VAILLON R. The multi-spectral reordering (MSR) technique for the narrow band modeling of the radiative properties of non-uniform gaseous paths: the correlated/uncorrelated approximations, *Journal of Physics: Conference Series* 369, 2012.
- [18] HU H, WANG Q. Improved MSMGFSK models apply to gas radiation heat transfer calculation of exhaust system of TBCC, *JHT* 2017 ;139,012702-1-11.
- [19] HU H, WANG Q. Improved spectral absorption coefficient grouping strategy of wide band k-distribution model used for calculation of infrared remote sensing of hot exhaust systems, *JQSRT* 2018;213:17-34.
- [20] NELSEN R.B. An introduction to Copulas - Second Edition, Springer series in statistics, Springer, 2006.
- [21] RIVIERE Ph, SOUFIANI A, TAINÉ J. Correlated-k fictitious gas model for H<sub>2</sub>O infrared radiation in the Voigt regime, *JQSRT* 1995;53:335-346.
- [22] FU Q, LIOU KN. On the correlated-k distribution method for radiative transfer in nonhomogeneous atmospheres, *Journal of Atmospheric Sciences* 1992;49:2139-2156.
- [23] ROTHMAN LS, GORDON LE, BARBER RJ, DOTHE H, GAMACHE RR, GOLDMAN A, PEREVALOV VI, TASHKUN SA, TENNYSON J. HITEMP, the high-temperature molecular spectroscopic database, *JQSRT* 2010;111:2139-2150.
- [24] ANDRE F. Effective scaling factors in non-uniform gas radiation modeling, *JQSRT* 2018;206:105-116.
- [25] ANDRE F. The  $\ell$ -distribution method for modeling non-gray absorption in uniform and non-uniform gaseous media, *JQSRT* 2016;179:19-32.